Delayed Wound Healing in Immunodeficient TGF-β1 Knockout Mice

Maria J. Crowe,*‡ Thomas Doetschman,† and David G. Greenhalgh§¶

Departments of *Surgery and †Molecular Genetics, Biochemistry & Microbiology, University of Cincinnati College of Medicine, Cincinnati, Ohio, U.S.A.; Shriners Hospitals for Children, ‡Cincinnati and §Northern California, ¶Department of Surgery, University of California, Davis, California, U.S.A.

Previous studies showed that full-thickness wounds in transforming growth factor-β1-deficient mice initially heal normally. Unfortunately, transforming growth factor-β1 deficiency leads to a multifocal inflammatory disease affecting most organs of the body, which ultimately interferes with later stages of wound healing in these mice. As this inflammatory disease is eliminated in transforming growth factor-β1-deficient mice lacking T and B cells (*Tgfb1*$^{-/-}$ *Scid*$^{-/-}$ mice), we hypothesized that wound repair in the latter would proceed normally, even at later stages of healing. Unexpectedly, *Tgfb1*$^{-/-}$ *Scid*$^{-/-}$ mice demonstrate a major delay of approximately 1 wk in each of the major phases of wound healing: inflammation, proliferation, and maturation. Immunodeficient *Scid*$^{-/-}$ mice that have the wild-type *Tgfb1* allele do not experience this delay in wound healing. One interpretation of these findings is that lymphocytes and transforming growth factor-β1 affect compensatory pathways in wound healing. An alternative interpretation is that the delayed expression of *Tgfb2* and *Tgfb3* that occurs in the absence of transforming growth factor-β1 results in the delayed wound healing, suggesting that transforming growth factor-β2 and/or transforming growth factor-β3 play important parts in wound healing. *Key words: gene expression/knockout mice/skin injury/transforming growth factor-β isoforms. J Invest Dermatol 115:3–11, 2000*

Tissue repair involves an orchestration of various cytokines and growth factors that result in a regular progression of re-modeling events. When tissue is destroyed by injury, the healing process proceeds through three phases: an inflammatory phase characterized by cell proliferation and migration; a proliferative phase dominated by collagen deposition and angiogenesis; and a maturation phase involving resolution of inflammation and scar maturation (Greenhalgh and Staley, 1993; Clark, 1996).

The multifunctional cytokine transforming growth factor-β (TGF-β), has been shown to play a part in all three phases of healing (Roberts *et al*, 1988). TGF-β1 is the prototypic member of a structurally related polypeptide family that is involved in many proliferative, inductive, and regulatory process (Roberts and Sporn, 1990). The three major mammalian TGF-β isoforms (TGF-β1, TGF-β2, and TGF-β3) are encoded by distinct genes (Roberts and Sporn, 1990) and share a 64–85% amino acid sequence similarity (Massagué, 1990). Even though they demonstrate both distinct and overlapping patterns of expression in development (Heine *et al*, 1987; Lehnert and Akhurst, 1988), the 30-plus knockout phenotypes of the *Tgfb1*, *Tgfb2*, and *Tgfb3* genes do not overlap (Shull *et al*, 1992; Kulkarni *et al*, 1993; Kaartinen *et al*, 1995; Proetzel *et al*, 1995; Sanford *et al*, 1997), indicating a wide range of nonredundant functions (Doetschman, 1999). As the prototypic member of the family, TGF-β1 has been characterized more extensively than the other two members. In the repair process, TGF-β1 is one of the first cytokines to elicit inflammatory cell recruitment. Initiation of the inflammatory phase is thought to be accomplished by the release of TGF-β1 and other growth factors from the α granules of degranulating platelets after tissue injury (Massagué, 1990). TGF-β1 can be chemotactic and mitogenic for neutrophils, lymphocytes, monocytes, macrophages, and fibroblasts (Postlethwaite *et al*, 1987; Wahl *et al*, 1987; Adams *et al*, 1991; Parekh *et al*, 1994). After they have migrated to the wound site, inflammatory cells synthesize and secrete additional TGF-β1, which at higher concentrations may induce the expression of other growth factors, thereby increasing the cellularity of the wound. The role of TGF-β1 during the proliferative phase of healing has been implicated by its demonstrated ability to stimulate angiogenesis (Roberts *et al*, 1986) and collagen deposition in normal and compromised tissue (Beck *et al*, 1991; Hosgood, 1993; Nall *et al*, 1996). In the maturation phase of healing, TGF-β1 may continue to exert control over extracellular matrix components, not only by promoting their production, but also by inhibiting the actions of those substances that would otherwise serve to break them down. Its control over extracellular matrix deposition has implicated TGF-β1 in scar formation (Shah *et al*, 1994).

In addition to its potentially important part in tissue repair, TGF-β1 is a potent regulator of the immune response (Wahl, 1992) and is generally immunosuppressive. It is the most potent known endogenous inhibitor of both B and T lymphocyte proliferation and differentiation, and it can alter the functions of all classes of mature leukocytes (Smeland *et al*, 1987; Rehman and LeBien, 1993; Wahl, 1994). Mice with targeted disruption of the *Tgfb1*

Manuscript received October 1, 1999; revised March 31, 2000; accepted for publication April 4, 2000.

Reprint requests to: Dr. Thomas Doetschman, Department of Molecular Genetics, Biochemistry & Microbiology, University of Cincinnati College of Medicine, 231 Bethesda Ave (ML 524), Cincinnati, OH 45267-0524. Email: thomas.doetschman@uc.edu

Abbreviations: TGF-β, transforming growth factor β (refers to the protein); *Tgfb*, transforming growth factor β (refers to the gene); *Scid*, severe combined immunodeficiency gene.

gene display a phenotype that suggests the loss of a critical regulator of immune function. These mice develop a multifocal inflammation, with massive infiltration of lymphocytes and macrophages into most major organ systems (Shull *et al*, 1992, 1994; Kulkarni *et al*, 1993; Diebold *et al*, 1995). The syndrome develops during the first postnatal week and culminates in death at about 3 wk of age. Elevated levels of peripheral lymphocytes and immature neutrophils as well as increased numbers of proliferating cells in spleens and lymph nodes are found in TGF-β1-deficient mice.

Even though TGF-β1 has been implicated in playing multiple parts in wound healing, largely because it was usually the only TGF-β investigated, it is not altogether clear which of the TGF-β ligands actually plays each of these parts. Indeed, previous studies on wound healing in 10 d old TGF-β1-deficient mice did not reveal any differences in healing between mutant and control mice (Brown *et al*, 1995; Letterio and Roberts, 1996) until the time when the animals began to succumb to the overwhelming proliferation of inflammatory cells; however, this probably has less to do with wound healing and more to do with the multifocal inflammation phenotype of the *Tgfb1* knockout mouse. These studies strongly suggested that TGF-β2 and/or TGF-β3 play an important part in wound healing.

To assess, more accurately, the interaction between lymphocytes and TGF-β1 during the tissue repair process, a mouse model was utilized that was both immunodeficient ($Scid^{-/-}$ lacking B and T lymphocytes) and TGF-β1 deficient. The immunodeficiency background eliminates the widespread inflammation that is normally seen in TGF-β1-deficient mice (Diebold *et al*, 1995), making it more possible to conduct a longer-term wound healing study.

We hypothesized that immunodeficient TGF-β1-deficient mice would provide a model in which to examine (i) the progress of wound healing in the absence of both TGF-β1 and excessive inflammation, and (ii) the ligand-specific effects of TGF-β on wound healing. This model shows that when combined, lymphocytes and TGF-β1 can play an important part in wound healing. It also demonstrates that in spite of some overlap in expression during wound healing, there is no apparent redundancy or compensation between TGF-β1 and either TGF-β2 or TGF-β3, and that TGF-β2 may be playing an initial part in wound healing.

MATERIALS AND METHODS

Generation of $Tgfb1^{-/-}$ $Scid^{-/-}$ mutants The generation of $Tgfb1^{-/-}$ $Scid^{-/-}$ immunodeficient double mutant mice has been described (Diebold *et al*, 1995). Briefly, a mouse genomic library was prepared and the *Tgfb1* gene was isolated. A targeting vector knocked out the *Tgfb1* gene in embryonic stem cells. Mice were genotyped using upstream and downstream primers corresponding to *Tgfb1* exon 6 sequences flanking the *neo* insert in the *Tgfb1*– null allele.

The homozygous mutant TGF-β1 knockout mice ($Tgfb1^{-/-}$) were born visibly indistinguishable from their littermates. By day 7 their growth slowed and by day 35, 98% of the mice died. Elevated inflammatory cytokines and elevated counts of monocytes and immature neutrophils were consistent with an inflammatory disorder (Shull *et al*, 1992, 1994). The *Tgfb1* mutation was put on the severe combined immunodeficiency ($Scid^{-/-}$) background in which there are no lymphocytes. Putting the *Tgfb1* knockout allele on the $Scid^{-/-}$ background eliminated the inflammatory disease (Diebold *et al*, 1995). By 70 d of age the double mutant animals showed no signs of the wasting phenotype that normally occurred by the third week of age in the immunocompetent *Tgfb1* knockout mice.

Genetic background *Tgfb1* knockout mouse colonies cannot be maintained on an inbred strain if they are to generate live births of $Tgfb1^{-/-}$ animals (Kallapur *et al*, 1999). Therefore, they must be maintained on a mixed background to carry out adult wound healing studies. Consequently, the $Tgfb1^{-/-}$ $Scid^{-/-}$ mouse colonies are maintained as advanced intercross lines so as to maintain the 12% 129S2/SvPas and 88% C3H background mixture without inadvertently generating recombinant inbred strains. Siblings are never intercrossed during maintenance of the lines, but siblings are always used as experimental controls in order to minimize genetic background differences. To meet the requirement that experimental controls be siblings, $Tgfb1^{+/-}$ $Scid^{-/-}$ animals were occasionally used as controls, as there was no apparent difference between them and $Tgfb1^{+/+}$ $Scid^{-/-}$ animals with respect to wound healing.

Wounding protocol $Tgfb1^{-/-}$ $Scid^{-/-}$ were used for the wounding experiments. Homozygous wild-type ($Tgfb1^{+/+}$ $Scid^{-/-}$) and heterozygous ($Tgfb1^{+/-}$ $Scid^{-/-}$) littermates were used as controls. A total of 23 females and 26 males were used for these experiments, and they were evenly distributed between the three genotypes used ($Tgfb1^{+/+}$, seven females and nine males; $Tgfb1^{+/-}$, eight females and seven males; $Tgfb1^{-/-}$, eight females and 10 males). There was no significant difference in wound healing characteristics between males and females so gender distinctions were not made. The animals were 8–10 wk old at the time of wounding. Mutant mice ranged from 12 to 15 g because for unknown reasons they are always smaller (Shull *et al*, 1992), and their littermate controls (whether $Tgfbl^{+/-}$ or $Tgfb1^{+/+}$ animals) ranged from 18 to 20 g. Mice were individually housed in microisolator cages in an isolated animal care facility devoid of known mouse pathogens. They were maintained on a 12 h light/12 h dark cycle and given free access to autoclaved mouse chow and sterilized water supplemented with antibiotics [sulfamethoxazole (0.25 mg per ml) and trimethoprim (0.09 mg per ml)].

All wounding was performed using aseptic conditions. Mice were anesthetized by methoxyflurane inhalation (Metofane, Mallinckrodt Veterinary, Mundelein, IL). The hair on the animal's back was shaved, and the wound site was washed with Povidone-iodine solution followed with 30% isopropyl alcohol. A template was used to delineate a 1×1 cm area on the mid back. A full-thickness wound corresponding to the template was created through the skin and panniculus carnosus. Tincture of benzoin (Cumberland-Swan, Smyrna, TN) was applied outside the perimeter of the wound and allowed to dry. The wound was covered with a semipermeable polyurethane nonabsorbent dressing (OpSite; Smith and Nephew Medical, Hull, U.K.) and sealed at the edges. The transparent OpSite dressing allowed for visualization of the wound edge for open wound area determinations.

Wound analysis For the evaluation of healing of the open, full-thickness wounds, repeated measures of the wound area were performed. At wounding, an outline of the original wound was made on a glass slide to determine the original wound area. This area at day 0 was used as a reference for determining the extent of wound closure over time. Wound edges were serially traced on to glass slides on day 0 and every 2 d for the duration of the survival period. Tracings were made through the OpSite while the animals were awake or lightly anesthetized with methoxyflurane. Wound tracing areas were measured by planimetry with the use of an image analysis system (Image-1, Universal Imaging, Media, PA). The wound areas were standardized by comparison with the original wound size, expressed as a percentage of wound closure: % wound closure = [(day 0 area − day N area)/day 0 area] × 100. The extent of wound contraction was visualized as the edge of scar and was easily distinguishable from the extent of re-epithelialization. Mice were killed on days 5, 10, 14, or 21 d postwounding by sodium pentobarbital overdose (200 mg per kg IP). After the final wound tracings were made, the entire wound, including a 5 mm margin of unwounded skin was excised down to the fascia. The wound was divided in half through the least healed portion. Half of the wound was fixed in 4% paraformaldehyde, embedded in paraffin and processed for histology. The other half was frozen in liquid nitrogen and stored at −70°C for molecular analysis.

Histology After the bisected wound was fixed, the specimen was mounted so that the midportion of the wound was cut in 5 μm sections. Hematoxylin and eosin stains were used for the evaluation of the basic architecture and cellularity. The histologic sections were given a histologic score ranging from 1 to 12 with 1 corresponding to no healing and 12 representing a completely healed wound. Scoring was based on the cellularity, granulation tissue formation, and epithelial travel in the wound. The histologic scoring system has been previously published and has proven to be a reliable method for assessing the degree of tissue repair based on histology (Greenhalgh *et al*, 1990). The wounds were evaluated by at least two investigators blinded to the genotype and length of survival time postinjury for each animal. The investigators' scores were combined and averaged for each animal. Masson's Trichrome stain (stains collagen blue) was used as a qualitative measure of the extent of collagen deposition.

Reverse transcriptase–polymerase chain reaction (RT–PCR) RT–PCR was used to detect the presence of the three *Tgfb* mRNA in the wounds. Frozen wound tissues were pooled by survival time and genotype in order to maximize yield. Tissues were ground into a powder using a

liquid nitrogen-cooled Bessman Stainless Steel Tissue Pulverizer (Fisher Scientific, Pittsburgh, PA). The powder was then homogenized with a Tissumizer apparatus (Tekmar-Dohrmann, Cincinnati, OH) in 1 ml of TriReagent Solution (Molecular Research Center, Cincinnati, OH). Total RNA was extracted from the homogenized tissues according to the TriReagent protocol. The purity and concentration (yield) of RNA was determined by spectrophotometry. Diluted RNA was electrophoresed on a 1% agarose gel (Life Technologies, Gaithersburg, MD), stained with 0.5 ng per ml ethidium bromide (Life Technologies), destained with distilled water, and viewed under ultraviolet light to determine RNA integrity. Total RNA was then diluted to 1 μg per μl with sterile diethylpyrocarbonate-treated water stored at –70°C until use.

A reverse transcriptase step was performed on the RNA to yield cDNA. An aliquot of RNA was diluted to 1 μg per μl and 2 μg were diluted in a total volume of 11 μl with diethylpyrocarbonate-treated water. One microliter of Oligo dT primer [Boehringer Mannheim, Indianapolis, IN (0.5 μg per μl)] was added to the RNA and the sample was heated to 90°C for 2 min and slowly cooled to 42°C over 60 min. The synthesis reaction was completed by adding 4 μl of 5 × Reaction Buffer, 2 μl of 0.1 M dithiothreitol, 1 μl of mixed dNTP stock (10 mM each of dATP, dGTP, dCTP, dTTP) and 1 μl (200 units) of reverse transcriptase and incubated at 42°C for 60 min. A DNA Thermocycler (Perkin Elmer, Foster City, CA) was used for all temperature regulation. To inactivate the enzyme, the tubes were then frozen at –70°C for at least 15 min. Primers specific for β-*actin*, *Tgfb1*, *Tgfb2*, and *Tgfb3* were produced by obtaining the proper oligonucleotide primer sequence from the literature and being synthesized by the DNA Core Facility located within the University of Cincinnati College of Medicine. The primers were obtained in the lyophilized form, then diluted with sterile double distilled water to 1 μg per μl and stored at –20°C until use. For PCR amplification, 2 μl of the cDNA was combined in a new PCR tube with 31.5 μl sterile, distilled water, 5 μl of 10 × PCR Buffer, 5 μl of 25 mM $MgCl_2$, 5 μl of 10 mM dNTP mix, 1 μl of each primer synthesized from the Core Facility (3′ and 5′) and 0.5 μl *Taq* polymerase (5 U per μl). The sample was covered with two drops of mineral oil to prevent evaporation. Amplification of cDNA was carried out with conditions specific for each of the primer sets:

Actb (β-actin)—540 bp (Knisely *et al*, 1991) (accession no. M12481)
5′ (forward) primer 5′-GTGGGCCGCTCTAGGCACCAA-3′ (nt25–45)
3′ (reverse) primer 5′-CTCTTTGATGTCACGCACGATTTC-3′ (nt541–564)
Amplification conditions: 94°C for 1 min, 60°C for 2 min, 72°C for 3 min, final extension 72°C for 7 min (35 cycles)

Tgfb1—682 bp (Knisely *et al*, 1991) [accession no. L42456 (forward); L42461 (reverse)]
5′ (forward) primer 5′-GCTAATGGTGGACCGCAACAACG-3′ (nt5224–5246)
3′ (reverse) primer 5′-CTTGCTGTACTGTGTGTCCAGGC-3′ (nt355–377)
Amplification conditions: 94°C for 1 min, 60°C for 2 min, 72°C for 3 min, final extension 72°C for 7 min (35 cycles)

Tgfb2—328 bp (Knisely *et al*, 1991) (accession no. X57413)
5′ (forward) primer 5′-CACCTCCCCTCCGAAAATGCCAT-3′ (nt1548–1570)
3′ (reverse) primer 5′-ACCCCAGGTTCCTGTCTTTGTGGT-3′ (nt1851–1875)
Amplification conditions: 94°C for 1 min, 60°C for 2 min, 72°C for 3 min, final extension 72°C for 7 min (35 cycles)

Tgfb3—636 bp (Proetzel *et al*, 1995) (accession no. M32745)
5′ (forward) primer 5′-GTCACTGACACTGTGCGCGA-3′ (nt1214–1233)
3′ (reverse) primer 5′-CTGGCCTCAGCTGCACTTAC-3′ (nt1830–1849)
Amplification conditions: 95°C for 25 s, 57°C for 50 s, 72°C for 90 s, final extension 72°C for 10 min (35 cycles)

Gel electrophoresis of the PCR products was performed on a 1% agarose gel. Positive and negative controls were used to confirm whether the PCR worked in each sample. The positive controls consisted of β-actin to ensure that the RNA was not degraded, and liver RNA to demonstrate that amplification of each *Tgfb* gave a signal. Every experiment was repeated and confirmed on pooled tissue samples from an independent experiment.

Quantitative RT–PCR To quantitate mRNA expression, a competitive RT–PCR technique was performed. A RT–PCR MIMIC construction kit (Clontech, Palo Alto, CA) was used to construct an internal standard, using the gene-specific primer sequences unique for each specific *Tgfb* cytokine (**Table I**) and corresponding composite primers (the gene-specific primer sequences with the ability to anneal with the neutral DNA fragment). An initial primary PCR amplification was performed using composite primers to make a product with the neutral DNA fragment. A secondary PCR amplification was then performed with the first product adding each gene-specific primer sequence to the ends. The final product consisted of the entire target primer sequence incorporated on to the ends of the neutral DNA fragment, resulting in an exogenous internal standard of a molecular weight different from the cytokine region to be amplified. This product was purified on a CHROMA SPIN + TE-100 column (Clontech), and quality of the PCR-MIMIC was checked on a 1.8% agarose gel. Estimation of PCR-MIMIC yield was determined by spectrophotometry. A portion was then diluted to 100 attomol per μl with ultrapure glycogen (50 μg per ml). Competitive RT–PCR was performed using the 100 attomol per μl working dilution of the internal standard. An initial 10-fold RT–PCR MIMIC dilution series was run, followed by a 2-fold dilution series using a starting dilution determined from the initial 10-fold dilution series.

Each RT–PCR product was subjected to a 1.8% agarose gel electrophoresis. The gel was stained with ethidium bromide, destained with distilled water, and viewed under ultraviolet light to identify bands of interest. A 100 bp DNA ladder (Life Technologies) was used as a size standard. Negative controls were run for each primer set to detect any contamination that may have occurred during either the reverse transcription or amplification reaction. Data presented in **Fig 5** are from RNA extractions and subsequent PCR analyses that were performed using tissues pooled from two to three mice/genotype. Error bars could not be used under these circumstances.

Apoptosis analysis in the wound Apoptotic cells were detected in paraffin-embedded wound sections by a modified TUNEL (Terminal Transferase dUTP Nick-End Labeling) reaction according to the following protocol: tissue sections were baked at 60°C for 30 min and then rehydrated by serial immersion for 5 min each in xylene (× 2), 100%, 95%, and 70% ethanol, deionized water and phosphate-buffered saline

Table I. Cross-regulation of *Tgfb2* and *Tgfb3* expression by TGFβ1[a]

Tgfb genotype (strain)[b]	Days after wounding								
	Tgfb1 expression			*Tgfb2* expression			*Tgfb3* expression		
	0	5	10	0	5	10	0	5	10
Tgfb1$^{+/+}$ *Scid*$^{-/-}$ (129S2/SvPas × C3H)	+	+	+	+	+	+	–	+	+
Tgfb1$^{+/-}$ *Scid*$^{-/-}$	+	+	+	+	+	+	–	+	+
Tgfb1$^{-/-}$ *Scid*$^{-/-}$	–	–	–	–	+	+	–	–	+
Tgfb1$^{+/+}$ (129S2/SvPas × CF-1)	+	+	+	+	+	+	+	nd	nd
Tgfb1$^{-/-}$	–	–	–	+	nd	+	+	nd	nd

[a]Data were compiled from two independent experiments, one of which is shown in detail in **Fig 5**. Positive and negative controls were used to confirm whether the PCR worked in each sample. The positive controls consisted of *β-actin* to ensure that the RNA was not degraded, and liver RNA to demonstrate that amplification of each *Tgfb* gave a signal.

[b]The Jackson Labs' revised nomenclature for 129 strains of mice is used here. The (129S2/SvPas × C3H) mice are approximately 12% 129S2/SvPas and 88% C3H backgrounds. The (129S2/SvPas × CF-1) mice are approximately 50% 129S2/SvPas and 50% C3H backgrounds. Each of these strains has been maintained at these levels of genetic mixture as ''Advanced Intercross Lines'' according to Jackson Labs' established procedures in order to prevent recombinant inbreeding of these lines (see Doetschman, 1999, for details).

(PBS). Sections were then covered with proteinase K (100 µl per slide of a 2 µg per ml solution in phosphate-buffered saline) and incubated in a humidifying chamber for 15 min, and washed with phosphate-buffered saline (5 min × 3). Tissue buffering was accomplished by a 1 min incubation with 1 × TdT buffer. A reaction "cocktail" was made using 100 µl of 5 × TdT buffer, 50 µl of fluorescein isothiocyanate-dUTP, 20 µl of TdT enzyme (0.5 U per ml) and 330 µl of deionized water. Slides were treated with 50 µl of "cocktail" per section and incubated at 37°C for 2.5 h in a humidifying chamber. Negative control sections were treated with the same cocktail, substituting deionized water for TdT enzyme. The reaction was stopped by bathing all slides in SSC (30 mM trisodium citrate and 300 mM sodium chloride) for 15 min at room temperature, followed by rinsing in phosphate-buffered saline for 5 min × 3. Coverslips were applied using an aqueous-based permanent mounting media (Crystal/Mount, Biomedia, Foster City, CA). Examination and photography were performed using a Nikon Microphot-FXA (Nikon, Melville, NY) equipped with an epifluorescence illumination system, and 400 ASA color slide film (Eastman Kodak, Rochester, NY).

Statistics Student's t test was used for comparisons of two groups. The extent of wound closure of multiple groups over time were compared using one-between, one-within repeated measures analysis of variance. Tukey's test was used for individual comparisons. The Kruskal–Wallis test with individual comparisons being performed by the Dunn's procedure was used for data involving ranking (i.e., histologic scores). The Wilcoxon rank-sum test was used for other nonparametric analyses. Data analysis was performed in conjunction with a statistician using SAS (version 6.04, SAS Institute, Cary, NC).

RESULTS

General wound healing As our previous study on *Tgfb1*$^{-/-}$ mice indicated a normal course of events in wound healing up to the time of resolution of the inflammatory response (Brown *et al*, 1995), we first measured wound closure to determine whether the additional absence of lymphocytes in *Tgfb1*$^{-/-}$ *Scid*$^{-/-}$ mice altered the progression of healing that was previously observed. A total of 18 mutants (*Tgfb1*$^{-/-}$ *Scid*$^{-/-}$), 15 heterozygous (*Tgfb1*$^{+/-}$ *Scid*$^{-/-}$), and 16 *Tgfb1* wild-type (*Tgfb1*$^{+/+}$ *Scid*$^{-/-}$) mice were used in the wounding study. Two of the mutants died within 3 d after wounding, but in general, the animals tolerated the procedures well, with 89% of the mutant mice and 100% of the control mice surviving to completion of the study. Preliminary experiments in our laboratory showed no appreciable differences in the rate of healing that occurred between the wild-type and heterozygous littermates (data not shown); therefore, they were used interchangeably as controls. Rapid healing was observed in the *Tgfb1*$^{+/+}$ *Scid*$^{-/-}$ and *Tgfb1*$^{+/-}$ *Scid*$^{-/-}$ animals, but a significant delay in wound closure was observed for the *Tgfb1*$^{-/-}$ *Scid*$^{-/-}$ animals by day 8 postwounding (**Fig 1**). Control animals reached almost 100% wound closure by day 16 whereas mutant animals never achieved complete wound closure during the course of this study which ended on day 21.

Histology Histologic comparison of the mutant and control wounds confirms that the defect in *Tgfb1*$^{-/-}$ *Scid*$^{-/-}$ mice appears to involve many components of wound healing. Representative hematoxylin and eosin-stained tissue sections are shown in **Fig 2**. Wounds from control *Scid*$^{-/-}$ littermates had typical cellular infiltration into the wounded tissue as early as 5 d postwounding (**Fig 2*a***). After high-power microscopic examination, these cells were identified as mainly nonlymphocytic inflammatory cells, primarily neutrophils and macrophages. The inflammatory response in the immunodeficient animals was robust despite the lack of functioning B and T lymphocytes genetically inherent to the *Scid*$^{-/-}$ mice. Angiogenesis was evident and re-epithelialization had begun in control wounds by day 5 (**Fig 2*a***). Wound healing in control mice progressed through the orderly development of a mature granulation tissue formation via proliferating inflammatory cells and fibroblasts, followed by collagen deposition (**Fig 2*c***, ***e***). By day 21, control wounds were well healed with complete re-epithelialization, as well as a decrease in overall cellularity and vascularization that is characteristic of wound maturation (**Fig 2*g***). There was a marked delay in cellular entry in wounds from *Tgfb1*$^{-/-}$ *Scid*$^{-/-}$ mutants, with significant numbers of inflammatory cells being absent until day 14 or later (**Fig 2*b***, ***d***, ***f***). Angiogenesis was not evident in mutant wounds until day 14 (**Fig 2*f***). Granulation tissue in day 21 mutant wounds was thin, less organized than controls, and displayed vascularization typical of control wounds at about day 10 (compare **Fig 2*c***, **Fig 2*h***). Using the histologic scoring system, it was clear that *Tgfb1*$^{-/-}$ *Scid*$^{-/-}$ wounds manifested an overall impairment of the wound healing process, evidenced by decreased inflammatory cell infiltration, granulation tissue formation and collagen deposition, compared with *Scid*$^{-/-}$ littermates with normal TGF-β1 (**Fig 3**).

Apoptosis Apoptosis has been shown to be involved in the normal downregulation and resolution of the inflammatory response to wounding (Brown *et al*, 1997). The onset of apoptosis after wounding was delayed in *Tgfb1*$^{-/-}$ *Scid*$^{-/-}$ mice compared with TGF-β1-producing *Scid*$^{-/-}$ littermates (**Fig 4*a***, ***b***). In the 5 d *Scid*$^{-/-}$ control wound, apoptosis was observed by the fluorescent labeling of cellular nuclei in granulation tissue that are presumed to be inflammatory cells (**Fig 4*a***). There was a marked increase in apoptosis by 10 d (**Fig 4*c***), which was concentrated in the granulation tissue beneath the leading epithelial edges. At 21 d postwounding, the concentration of apoptotic cells was greatly decreased. As wounds matured, less apoptotic cells were observed in the granulation tissue (**Fig 4*e***). In wounds of *Tgfb1*$^{-/-}$ *Scid*$^{-/-}$ animals, no apoptotic cells were noted at 5 d postwounding, although a minimal number of cells had migrated into the wound (**Fig 4*b***). Increased cellular infiltration was seen at 10 d, but the appearance of apoptotic cells was lacking (**Fig 4*d***). The first evidence of apoptosis in *Tgfb1*$^{-/-}$ *Scid*$^{-/-}$ wounds was observed at 14 d (data not shown). This low level remained nearly constant, until about 3 wk postwounding. At 21 d, significantly increased levels of apoptosis were seen in *Tgfb1*$^{-/-}$ *Scid*$^{-/-}$ wounds relative to earlier time points (**Fig 4*f***). When apoptosis patterns in the *Tgfb1*$^{-/-}$ *Scid*$^{-/-}$ and control wounds were compared, the control wounds were observed to exhibit greater amounts of apoptotic cells at an earlier time in the healing process. The localization of apoptotic cells within mutant wounds was different compared with controls. Apoptotic cells in control wounds were clustered in the granulation tissue beneath the advancing epithelial edge over the wound during early wound healing (days 5–14). In contrast, the location of apoptotic cells in mutant wounds was less organized and seemed to be randomly scattered throughout the granulation tissue (**Fig 4*f***).

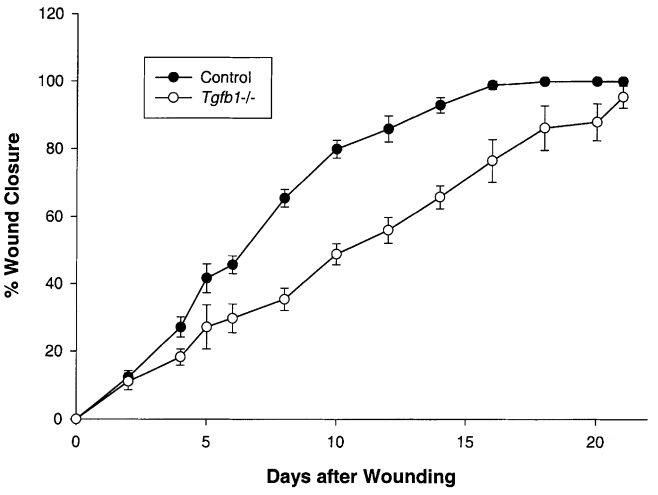

Figure 1. Wound closure in *Tgfb1*$^{-/-}$ *Scid*$^{-/-}$ and control mice. Significant differences ($p < 0.05$) in wound closure were observed between control and mutant animals by day 8 (by repeated measures analysis of variance). Control animals reached almost 100% wound closure by day 16, whereas mutant animals had not yet reached 100% wound closure by the endpoint of the experiment.

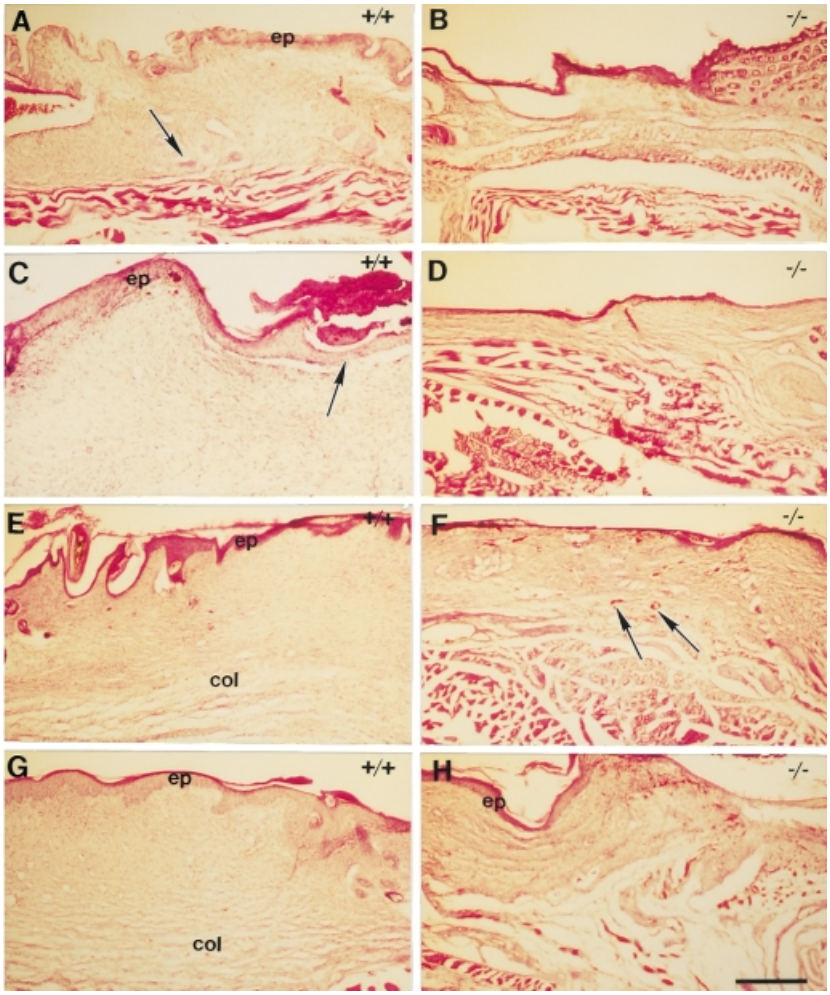

Figure 2. Histology of control and mutant wounds. At 5–10 d postwounding, control wounds (+/+ genotype) demonstrate a typical response (*A*, *C*) consisting of numerous invading inflammatory cells, areas of angiogenesis (*arrow* in *A*) and epithelial migration (*arrow* in *C*). In contrast, day 5–10 mutant wounds (–/– genotype) display very little evidence of inflammation, no angiogenesis and diminished epithelialization (*B*, *D*). Day 14–21 control wounds have a thick granulation tissue base and regular collagen deposition (*E*, *G*). Angiogenic sites are first evident in mutant wounds at 14 d postwounding (*arrows* in *F*). The mutant wound granulation tissue base is diminished and irregularly shaped (*H*) compared with control (*G*). *Scale bar*: 130 μm. ep, new epithelium; col, collagen deposition in maturing wound bed.

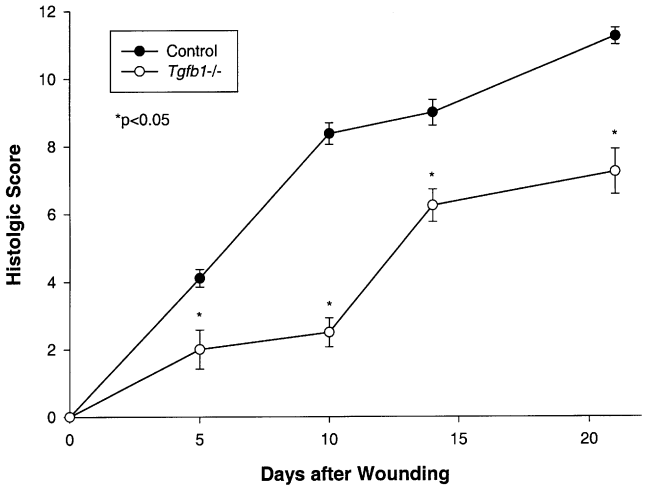

Figure 3. Histologic scores of *Tgfb1*$^{-/-}$ *Scid*$^{-/-}$ and control wounds. Scoring system developed by Greenhalgh *et al*, 1990 where 1 = no healing and 12 = complete healing. Significant differences ($p < 0.05$) in histologic score assessment were observed between control and *Tgfb1*$^{-/-}$ *Scid*$^{-/-}$ animals by day 5 (by Wilcoxon Rank Sum test). By day 21, control animals had achieved a score of 11.25 on a 12-point scale, whereas *Tgfb1*$^{-/-}$ *Scid*$^{-/-}$ animals had scored only 7.25.

Expression of *Tgfb* gene family members It is known that there is considerable overlap in expression between the three *Tgfb* genes, and that all three TGF-β isoform have some common receptor and signaling components. As many wounding studies involving TGF-β have not distinguished between the three closely related peptide factors, it was necessary to follow the expression patterns of *Tgfb2* and *Tgfb3* in wounds of *Tgfb1*$^{-/-}$ *Scid*$^{-/-}$ mice and their controls to determine whether there is any evidence for functional redundancy between TGF-β1 and its other two family members. Total RNA was isolated from day 0 unwounded skin and day 5, 10, 14, and 21 wounds. Liver tissue was used as a systemic control. RT–PCR was performed to detect transcripts for *Tgfb1*, *Tgfb2*, and *Tgfb3*. β-*actin,* which is ubiquitously expressed, was used as a positive control. Competitive RT–PCR was used to quantitate the amount of transcripts present in the unwounded and wounded skin samples. PCR reactions for each primer set were repeated at least four times to verify reproducibility of results. As expected, *Tgfb1* mRNA was detected in unwounded skin, liver, and wound tissues from *Tgfb1*$^{+/+}$ *Scid*$^{-/-}$ and *Tgfb1*$^{+/-}$ *Scid*$^{-/-}$ mice only (**Fig 5*a***, data for liver not shown). mRNA expression increased after wounding in skin tissues from both genotypes, with peak levels observed at 10–14 d postwounding. *Tgfb1* mRNA levels decreased to prewounding levels by day 21.

Tgfb2 mRNA was detected in *Tgfb1*$^{+/+}$ *Scid*$^{-/-}$ and *Tgfb1*$^{+/-}$ *Scid*$^{-/-}$ skin tissues, but was not present in *Tgfb1*$^{-/-}$ *Scid*$^{-/-}$ skin tissues at day 0 (**Fig 5*b***). *Tgfb2* mRNA was detected in liver tissues in all genotypes at all times examined (not shown). Upregulation of *Tgfb2* mRNA expression was observed in *Tgfb1*$^{-/-}$ *Scid*$^{-/-}$ skin tissue by day 5, with peak levels observed at day 14 postinjury; however, the degree of upregulation of mRNA expression did not significantly differ from that seen in *Tgfb1*$^{+/+}$ *Scid*$^{-/-}$ and *Tgfb1*$^{+/-}$ *Scid*$^{-/-}$ mice.

Tgfb3 mRNA was undetectable in skin tissues from all three genotypes at day 0 (**Fig 5*c***). It was detectable in liver tissues in all

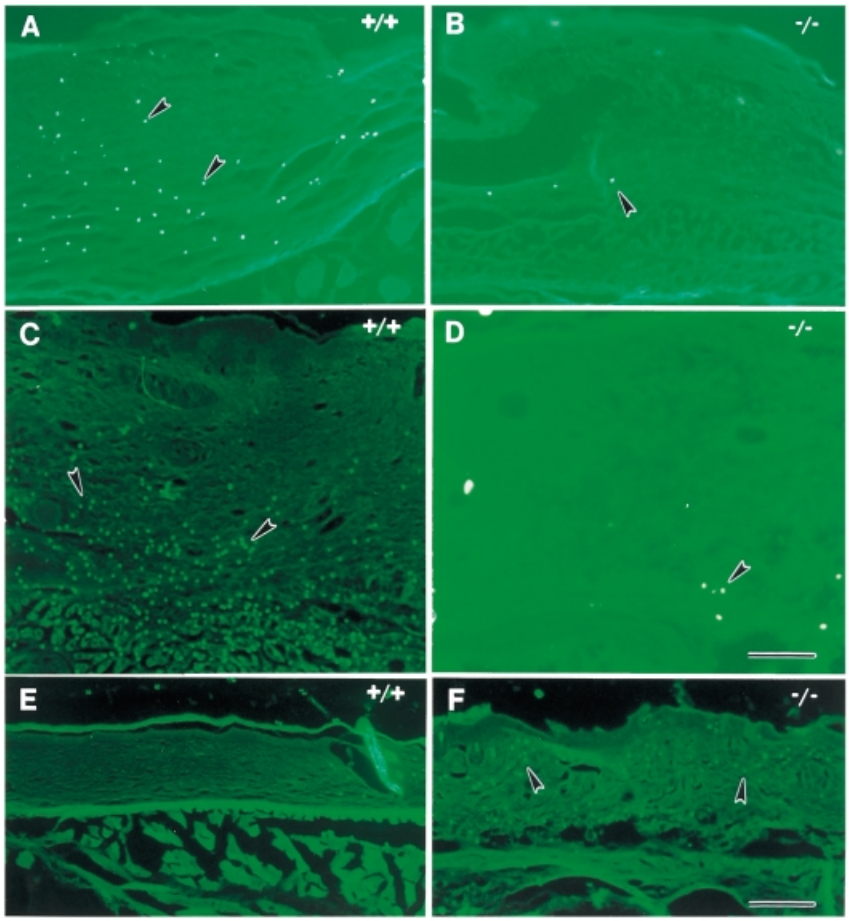

Figure 4. Apoptosis in wounds from control and *Tgfb1*$^{-/-}$ *Scid*$^{-/-}$ mice. Numerous TUNEL-labeled apoptotic cells are visible in control (+/+ genotype) wounds at 5 d (*A*) and 10 d (*C*) post-wounding. Apoptotic cells are located in the granulation tissue beneath the leading epithelial edge (e.g., *arrowheads* in *A* and *C*). By 21 d postwounding, few apoptotic cells are detected in control wounds (*E*). Very little labeling of apoptotic cells was observed within *Tgfb1*$^{-/-}$ *Scid*$^{-/-}$ wounds at early (5 d; *arrowhead* in *B*) or middle (10 d; *arrowhead* in *D*) time points after injury. At 21 d postwounding, numerous apoptotic profiles are seen scattered throughout the wound bed (e.g., *arrowheads* in *F*), indicating a delay in the onset of apoptosis relative to control wounds. *Scale bar*: (*A–D*) 130 μm; (*E*, *F*) 300 μm.

genotypes at all times examined (not shown). *Tgfb3* mRNA was upregulated in *Tgfb1*$^{+/+}$ *Scid*$^{-/-}$ and *Tgfb1*$^{+/-}$ *Scid*$^{-/-}$ skin tissues at 5 d postinjury, but was not detectable in *Tgfb1*$^{-/-}$ *Scid*$^{-/-}$ skin tissues until day 10. Interestingly, the amount of *Tgfb3* mRNA expression fell much more rapidly over time in *Tgfb1*$^{+/-}$ *Scid*$^{-/-}$ and *Tgfb1*$^{-/-}$ *Scid*$^{-/-}$ tissues than in *Tgfb1*$^{+/+}$ *Scid*$^{-/-}$ tissues.

DISCUSSION

In addition to numerous other physiologic functions, TGF-β1 is a potent regulator of the immune and inflammatory systems, and plays an important part in tissue repair. Two previous studies on *Tgfb1* knockout mice, however, indicated that only the resolution of the inflammatory response during wound repair is mediated by TGF-β1, and that other tissue repair functions previously attributed to TGF-β1 may instead be carried out by TGF-β2 and/or TGF-β3 (Brown *et al*, 1995; Letterio and Roberts, 1996). The complicating factor in those two studies was that the inflammatory phase of normal wound repair was exacerbated by the inherent multifocal inflammatory disease in the *Tgfb1* knockout mice, although an attempt was made to inhibit the inflammation in one of those studies (Letterio and Roberts, 1996). Consequently, we have repeated wound repair studies in animals completely rescued from the inflammatory disorder through genetic combination of the *Tgfb1* knockout gene with the *Scid* immunodeficiency gene (Diebold *et al*, 1995), thereby allowing an unfettered look at the effects of a total deficiency inTGF-β1 during tissue repair. After excisional injury to *Tgfb1*$^{+/+}$ *Scid*$^{-/-}$ mice, many inflammatory cells are recruited to the injury site. These animals heal well, suggesting that lymphocytes are not essential for relatively normal tissue repair as long as TGF-β1 is present. No appreciable differences in the rate or quality of healing are observed between heterozygous and wild-type control mice, suggesting that a single copy of the *Tgfb1* gene is sufficient to result in normal healing. Wounds from *Tgfb1*$^{-/-}$ *Scid*$^{-/-}$ animals exhibit a delayed and diminished inflammatory response compared with *Tgfb1*$^{+/+}$ *Scid*$^{-/-}$ control wounds, although vascularization and re-epithelialization do eventually occur. The delay in the inflammatory response continues with an impairment of the later phases of healing; collagen deposition and angiogenesis are similarly deficient.

The resolution of the inflammatory response to tissue injury and the decrease in cellularity that occurs during wound maturation has been shown to involve apoptosis (Desmouliere *et al*, 1996; Brown *et al*, 1997). Apoptosis (Buja *et al*, 1993; Schwartzman and Cidlowski, 1993; Williams and Smith, 1993; Stewart, 1994; Ueda and Shah, 1994) is believed to be one of the mechanisms whereby the hypercellularity of the wound is decreased as wound maturation proceeds. The signal for initiation of apoptosis in cells participating in the inflammatory response to wound healing is unknown, but has been speculated to originate from the leading edge of the migrating epithelium (Brown *et al*, 1997). This hypothesis was based on the consistent localization of apoptotic cells in the granulation tissue beneath the advancing epithelial edge. Results on the localization of apoptotic cells in control wounds in this study are consistent with that previous study. Localization of apoptotic cells in *Tgfb1*$^{-/-}$ *Scid*$^{-/-}$ wounds is delayed and random, however, indicating loss of a synchronized signal to those cell populations destined to undergo programmed cell death during the wound healing process. Because TGF-β1 has been shown to play a part in some apoptotic processes (Kyprianou and Isaacs, 1989; Oberhammer *et al*, 1992; Yanagihara and Tsumuraya, 1992; Yonish-Rouach *et al*, 1993), and as TGF-β1 is a regulator of the

inflammatory response to wounding, it was not surprising that resolution of the inflammatory response after wounding was disrupted and delayed in *Tgfb1*$^{-/-}$ *Scid*$^{-/-}$ mice.

Instances of severe tissue injury, such as those resulting from burns, have been shown to result in profound immunosuppression both in humans (Munster, 1976) and in animal models (Kupper and Green, 1984; Moss *et al*, 1988). Impaired neutrophil function, decreased lymphocyte blastogenesis, and the presence of circulating suppressive factors have been implicated in the pathophysiology of immunodepression related to burn tissue injury. The demonstrated control that TGF-β1 exerts on lymphocyte populations implicates at least a partial role for this cytokine in systemic immunodepression. From this study it is clear that an important interaction between lymphocytes and TGF-β1 must occur in order to bring about normal tissue repair and to hold inflammation in check in response to injury.

Given these observations, what roles can be attributed to TGF-β1 in wound healing? At first glance, some of the results presented here appear inconsistent with previously published results (Brown *et al*, 1995). The absence of just TGF-β1 does not lead to an initial delay in wound healing. Nor does the absence of just lymphocytes delay wound healing. Yet in the absence of both there is a significant delay. One interpretation of these results is that TGF-β1 and lymphocytes have compensatory parts to play on cells involved in the repair process. This is not so unreasonable given the multifunctional effects of both TGF-β1 and lymphocytes on the growth, differentiation, and function of other cell types, in particular, neutrophils and monocytes. For example, TGF-β1 and lymphocytes can enhance the initiation of inflammatory activity of macrophages through monocyte recruitment (Wahl *et al*, 1987) and macrophage activation (Kelso *et al*, 1982). Consequently, it is plausible that TGF-β1 and lymphocytes play an early, redundant part in initiating the wounding process, and that TGF-β1 functions later resolve the normal inflammatory response that occurs during wound repair.

Another interpretation of the data is that TGF-β2 and/or TGF-β3, rather than TGF-β1, function early in wound healing to ensure that the healing process occurs in a timely manner. Unlike the immunodeficient *Tgfb1*$^{-/-}$ *Scid*$^{-/-}$ mice studied here, the immunocompetent *Tgfb1*$^{-/-}$ mice studied previously (Brown *et al*, 1995) had no alteration in the expression of *Tgfb2* in the prewounded skin relative to its expression in wild-type mice. Analysis of *Tgfb3* expression in the skin of prewounded immunocompetent *Tgfb1*$^{-/-}$ mice also shows no downregulation of *Tgfb3* expression in the absence of TGF-β1 (summarized in the **Table I**). These differences in positive regulation of the expression of *Tgfb2* and *Tgfb3* by TGF-β1 appear to be mouse background specific. Other studies have indicated roles for TGF-β2 and TGF-β3 in wound repair. Inhibition of TGF-β2 activity (Shah *et al*, 1995; Wang *et al*, 1999) and addition of TGF-β3 (Shah *et al*, 1995) have been found to reduce collagen production and scarring; and TGF-β3, along with TGF-β1, have been found to induce myofibroblast contraction in fetal excisional wounds (Lanning *et al*, 2000).

These data do not rule out the possibility that delayed expression of *Tgfb2* and *Tgfb3* are the result, rather than the cause of some aspects of the delay in wound healing. Although later events during the healing process could be explained in this way, the absence of PCR-detectable *Tgfb2* and *Tgfb3* expression in prewounded mice cannot. In reality, both situations may occur: the absence of *Tgfb2* and *Tgfb3* expression may initially affect the healing process, and the subsequent healing response may in turn affect the expression of

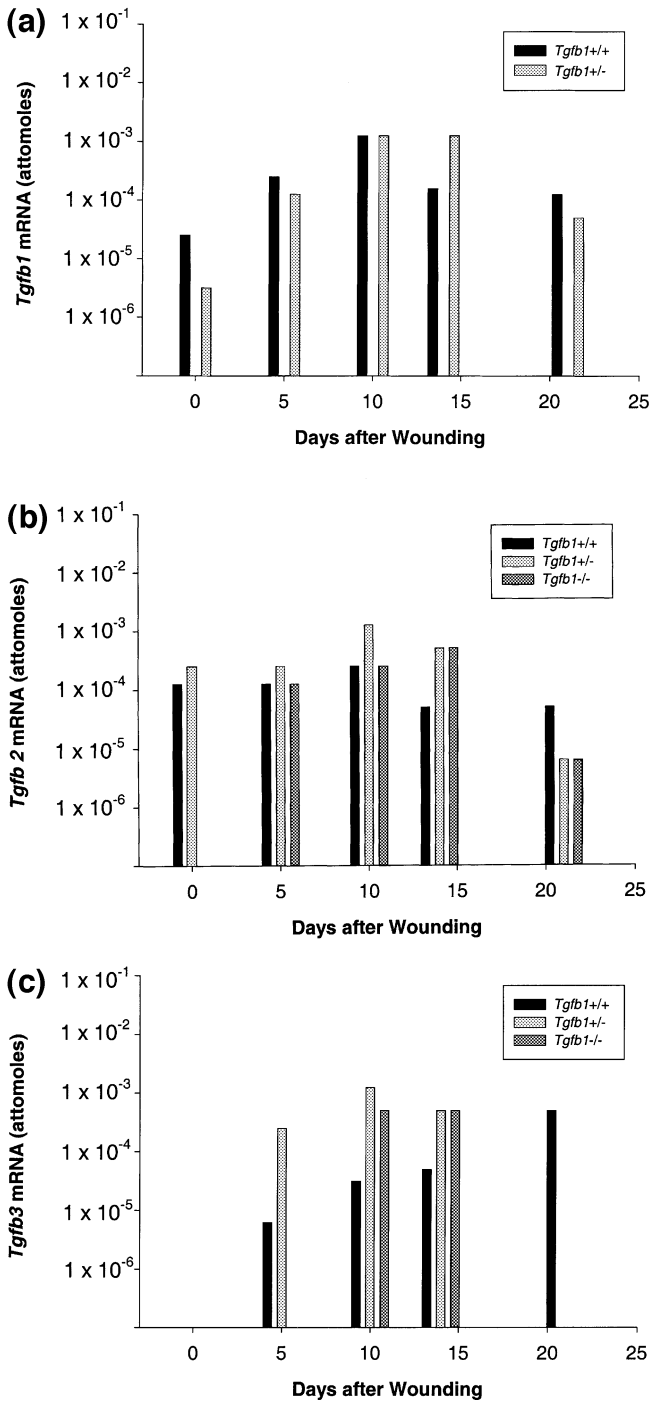

Figure 5. Concentration of *Tgfb* mRNA in wounds. (*a*) *Tgfb1* mRNA was detected in skin and wound tissues from heterozygous (+/–) and wild-type (+/+) *Scid*$^{-/-}$ mice only. mRNA expression increased after wounding in tissues from both genotypes, with peak levels observed at 10–14 d postwounding. *Tgfb1* mRNA levels decreased to prewounding levels by day 21. (*b*) *Tgfb2* mRNA was detected in *Tgfb1*$^{+/+}$ *Scid*$^{-/-}$ and *Tgfb1*$^{+/-}$ *Scid*$^{-/-}$ skin tissues, but was not present in *Tgfb1*$^{-/-}$ *Scid*$^{-/-}$ skin tissues at day 0. Upregulation of *Tgfb2* mRNA expression was observed in *Tgfb1*$^{-/-}$ *Scid*$^{-/-}$ tissues by day 5, with peak levels observed at day 14 postinjury. (*c*) *Tgfb3* mRNA was undetectable in skin tissues from all three genotypes at day 0. It was upregulated in *Tgfb1*$^{+/+}$ *Scid*$^{-/-}$ and *Tgfb1*$^{+/-}$ *Scid*$^{-/-}$ tissues at 5 d postinjury, but was not detectable in *Tgfb1*$^{-/-}$ *Scid*$^{-/-}$ tissues until day 10. The degree of upregulation of *Tgfb3* in *Tgfb1*$^{-/-}$ *Scid*$^{-/-}$ mice did not appear to be compensatory compared with the (+/+) and (+/–) *Scid*$^{-/-}$ genotypes. Each sample was pooled from three different animals, and PCR reactions for each primer set were repeated at least four times to verify reproducibility of results. Positive and negative controls were used to confirm whether the PCR worked in each sample. The positive controls consisted of *β-actin* to ensure that the RNA was not degraded, and liver RNA to demonstrate that amplification of each *Tgfb* gave a signal. Data from pooled samples from an independent experiment confirmed the results shown here.

Tgfb2 and *Tgfb3*, although wound responses generally led to the upregulation (Querfeld *et al*, 1999) and activation (Yang *et al*, 1999) of TGF-β, rather than the opposite. Definitive determination of the functions of the three TGF-β in wound healing awaits conditional knockouts of these genes.

Unexpected strain differences in the cross-family regulation of *Tgfb2* and *Tgfb3* expression by TGF-β1 have led to the observation that there is a delay in the healing process only in the TGF-β1-deficient strain in which there was no *Tgfb2* and *Tgfb3* expression at the time of wounding. Hence, the absence of TGF-β2 and/or TGF-β3, rather than TGF-β1, may actually result in the initial delay in wound healing in immunodeficient $Tgfb1^{-/-}$ $Scid^{-/-}$ mice. Conversely, the presence of TGF-β2 and TGF-β3 in immunocompetent $Tgfb1^{-/-}$ mice may have allowed healing to occur without initial delay.

In this study the expression pattern of *Tgfb3* is unlike that of *Tgfb2*. *Tgfb3* is not expressed in unwounded skin, regardless of the presence or absence of TGF-β1. At 5 d postwounding, however, it is still not present in the $Tgfb1^{-/-}$ $Scid^{-/-}$ mice; whereas, it is present in $Tgfb1^{+/+}$ and $Tgfb1^{+/-}$ $Scid^{-/-}$ mice. In the $Tgfb1^{-/-}$ animals used in a previous study (Brown *et al*, 1995) there is *Tgfb3* expression in unwounded skin (data not shown). Consequently, the absence of TGF-β3 does not correlate with the initial delay in healing, but rather correlates with the delay at about 5 d postwounding. The more rapid loss of *Tgfb3* expression in $Tgfb1^{+/-}$ $Scid^{-/-}$ than in $Tgfb1^{+/+}$ $Scid^{-/-}$ mice (day 20, **Fig 5*c***), cannot easily be explained, as no other differences were found between $Tgfb1^{+/+}$ and $Tgfb1^{+/-}$ $Scid^{-/-}$ mice. As this early loss of *Tgfb3* expression occurs between 2 and 3 wk postwounding, however, it does not detract from the observation that a healing delay of about 1 wk, and the delayed expression of *Tgfb3* for about 1 wk, are temporally correlated. These results are consistent with previous suggestions (Brown *et al*, 1995; Letterio and Roberts, 1996) that TGF-β isoforms other than TGF-β1, may be playing an important part in the early stages of wound healing.

To summarize, the expression data suggest that TGF-β2 can compensate for TGF-β1 during the first few days of healing, and that TGF-β3 can compensate for TGF-β1 after the first few days. TGF-β2, however, is unable to compensate for the loss of TGF-β3 after the first few days of healing. Together, these data lend credence to the hypothesis that the different TGF-β isoforms play both distinct and nonredundant functions during wound healing. Unfortunately, as *Tgfb2* and *Tgfb3* knockout mice die at birth due to severe congenital defects (Proetzel *et al*, 1995; Sanford *et al*, 1997), it is not presently possible to use them to confirm definitively these interpretations. Previous studies demonstrated that TGF-β1 is essential for resolving the inflammatory process involved in wound healing. This study provides two possible interpretations concerning additional roles of TGF-β isoforms in wound healing. The first involves a compensatory role between TGF-β1 and lymphocytes in ensuring that wound healing occurs in a timely process. The second suggests that TGF-β2 and/or TGF-β3, rather than TGF-β1, are the TGF-β involved initially in wound healing. Resolutions of these interpretations await the development of *Tgfb2* and *Tgfb3* knockout strains that survive their perinatal lethalities.

The authors would like to thank Ilona Ormsby and Christine Kane for excellent technical support, and Laura James for help with statistical analysis. This study was made possible by the following grant support: NIH ROI GM50959, ROI HD26471 and the Shriners of North America.

REFERENCES

Adams DH, Hathaway DM, Shaw J, Bumett D, Elias E, Strain AJ: Transforming growth factor-β induces T lymphocyte migration in vitro. *J Immunol* 147:609–612, 1991

Beck LS, Deguzman L, Lee WP, Xu Y, McFatride L, Amento EP: TGF-β1 accelerates wound healing: reversal of steroid-impaired healing in rats and rabbits. *Growth Factors* 5:295–304, 1991

Brown DL, Kao WW-Y, Greenhalgh DG: Apoptosis down-regulates inflammation under the advancing epithelial wound edge: Delayed patterns in diabetes and improvement with topical growth factors. *Surgery* 121:372–380, 1997

Brown RL, Ormsby I, Doetschman TC, Greenhalgh DG: Wound healing in the transforming growth factor-β1-deficient mouse. *Wound Rep Reg* 3:25–36, 1995

Buja LM, Eigenbrodt ML, Eigenbrodt EH: Apoptosis and necrosis. Basic types and mechanisms of cell death. *Arch Pathol Lab Med* 117:1208–1214, 1993

Clark RAF. Wound repair—overview and general considerations. In: Dark RAF (ed.). *The Molecular and Cellular Biology of Wound Repair*. New York: Plenum Press, 1996, pp 3–50

Desmouliere A, Redard M, Darby I, Gabbiani G: Apoptosis mediates the decrease in cellularity during the transition between granulation tissue and scar. *Am J Pathol* 146:56–66, 1996

Diebold RJ, Eis MJ, Yin M, *et al*: Early-onset multifocal inflammation in the transforming growth factor-β1-null mouse is lymphocyte mediated. *Proc Natl Acad Sci USA* 92:12215–12219, 1995

Doetschman T: Interpretation of phenotype in genetically engineered mice. *Laboratory Anim Sci* 49:137–143, 1999

Greenhalgh DG, Staley MJ. Burn wound healing. In: Richard RL, Staley MJ (eds). *Burn Care and Rehabilitation: Principles and Practice*. Philadelphia, PA: FA Davis Co., 1993, pp 70–102

Greenhalgh DG, Sprugel KH, Murray MJ, Ross R: PDGF and FGF stimulate wound healing in the genetically diabetic mouse. *Am J Pathol* 136:1235–1246, 1990

Heine UI, Munoz EF, Flanders KC, *et al*: Role of the transforming growth factor-beta in the development of the mouse embryo. *J Cell Biol* 105:2861–2876, 1987

Hosgood G: Wound healing—Role of platelet-derived growth factor and transforming growth factor-beta. [Review] *Vet Surg* 22:490–495, 1993

Kaartinen V, Voncken JW, Shuler C, Warburton D, Bu D, Heisterkamp N, Groffen J: Abnormal lung development and cleft palate in mice lacking TGF-beta 3 indicates defects of epithelial–mesenchymal interaction. *Nature Genet* 11:415–421, 1995

Kallapur S, Ormsby I, Doetschman T: Strain dependency of TGF-β1 function during embryogenesis. *Mol Reprod Dev* 52:341–349, 1999

Kelso A, Glasebrook AL, Kanagawa O, Brunner KT: Production of macrophage-activating factor by T lymphocyte clones and correlation with other lymphokine activities. *J Immunol* 129:550–556, 1982

Knisely TL, Bleicher PA, Vibbard CA, Granstein RD: Production of latent transforming growth factor-beta and other inhibitory factors by cultured murine iris and ciliary body cells. *Curr Eye Res* 10:761–771, 1991

Kulkarni AB, Hub CG, Becker B, *et al*: Transforming growth factor beta 1 null mutation in mice causes excessive inflammatory response and early death. *Proc Natl Acad Sci USA* 90:770–774, 1993

Kupper TS, Green DR: Immunoregulation after thermal injury: sequential appearance of l-J+, Ly-I T suppressor inducer cells and Ly-2 T suppressor effector cells following thermal trauma in mice. *J Immunol* 135:3053–3050, 1984

Kyprianou N, Isaacs JT: Expression of transforming growth factor-β in the rat ventral prostate programmed cell death. *Mol Endocrinol* 89:1515–1522, 1989

Lanning DA, Diegelmann RF, Yager DR, Wallace ML, Bagwell CE, Haynes JH: Myofibroblast induction with transforming growth factor-betal and -beta3 in cutaneous fetal excisional wounds. *J Pediatr Surg* 35:183–187, 2000

Lehnert SA, Akhurst RJ: Embryonic expression pattern of TGF-beta type-1 RNA suggests both paracrine and autocrine mechanisms of action. *Development* 104:263–272, 1988

Letterio JJ, Roberts AB: Transforming growth factor-β1-deficient mice: identification of isoform-specific activities in vivo. *J Leukoc Biol* 59:769–774, 1996

Massagué J: The transforming growth factor-β family. *Annu Rev Cell Biol* 6:597–641, 1990

Moss MM, Gough DB, Jordan AL: Temporal correlation of impaired immune response after thermal injury with susceptibility to infection in a murine model. *Surgery* 104:882–887, 1988

Munster AM: Post-traumatic immunosuppression is due to activation of suppressor T cells. *Lancet* i:1329–1330, 1976

Nall AV, Brownlee RE, Colvin CP, *et al*: Transforming growth factor beta 1 improves wound healing and random flap survival in normal and irradiated rats. *Arch Otolaryngol* 122:171–177, 1996

Oberhammer FA, Pavelka M, Sharms S, Tiefenbacher R, Purchio AF, Bursch W, Schulte-Hermann R: Induction of apoptosis in cultured hepatocytes and in regressing liver by transforming growth factor 131. *Proc Natl Acad Sci USA* 89:5408–5412, 1992

Parekh T, Saxena B, Reibrnan J, Cronstein BN, Gold LI: Neutrophil chemotaxis in response to TGF-β isoforms (TGF-β1, TGF-β2, and TGF-β3). *J Immunol* 152:2456–2466, 1994

Postlethwaite AE, Keski-Oja J, Moses HL, Kang AH: Stimulation of the chemotactic migration of human fibroblasts by transforming growth factor-β. *J Exp Med* 165:251–256, 1987

Proetzel G, Pawlowski S, Yin M, *et al*: Transforming growth factor-β3 is required for secondary palate fusion. *Nature Genet* 11:409–414, 1995

Querfeld C, Eckes B, Huerkamp C, Krieg T, Sollberg S: Expression of TGF-beta 1, -beta 2 and -beta 3 in localized and systemic scleroderma. *J Dermatol Sci* 21:13–22, 1999

Rehman JA, LeBien TW: Transforming growth factor-β regulates normal human pre-B cell differentiation. *Int Immunol* 6:315–322, 1993

Roberts AB, Sporn MB. The transforming growth factors-β. In: Sporn MB, Roberts AB (eds). *Peptide Growth Factors and Their Receptors*. Berlin: Springer-Verlag, 1990, pp 419–472

Roberts AB, Sporn MB, Assoian RK, *et al*: Transforming growth factor β: rapid induction of fibrosis and angiogenesis *in vivo* and stimulation of collagen formation *in vitro*. *Proc Natl Acad Sci USA* 83:4167–4171, 1986

Roberts AB, Flanders KC, Kondaiah P, *et al*: Transforming growth factor P. biochemistry and roles in embryogenesis, tissue repair and remodeling, and carcinogenesis. *Recent Prog Horm Res* 44:157–197, 1988

Sanford LP, Ormsby I, Gittenberger-de Groot AC, *et al*: TGFβ2 knockout mice have multiple developmental defects that are non overlapping with other TGFβ knockout phenotypes. *Dev* 124:2659–2670, 1997

Schwartzman RA, Cidlowski JA: Apoptosis: The biochemistry and molecular biology of programmed cell death. *Endocr Rev* 14:133–151, 1993

Shah M, Foreman DM, Ferguson MWJ: Neutralising antibody to TGF-β1,2 reduces cutaneous scarring in adult rodents. *J Cell Sci* 107:1137–1157, 1994

Shah M, Foreman DM, Ferguson MWJ: Neutralisation of TGFβ_1 and TGFβ_2, or exogenous addition of TGFβ_3, to cutaneous rat wounds reduces scarring. *J Cell Sci* 108:985–1002, 1995

Shull MM, Ormsby I, Kier A, *et al*: Targeted disruption of the murine TGFβ1 gene results in multifocal inflammatory disease. *Nature* 359:693–699, 1992

Shull MM, Kier A, Diebold RJ, Yin M-Y, Doetschman T. The importance of transforming growth factor β1 in immunological homeostasis as revealed by gene ablation in mice. In: Jacob C (ed.) *Overexpression and Knockout of Cytokine in Transgenic Mice*. London: Academic Press, 1994, pp 135–159

Smeland EB, Blomhoff HK, Holte H, *et al*: Transforming growth factor beta (TGF-β) inhibits Gl to S transition, but not activation of human B lymphocytes. *Exp Cell Res* 171:213–222, 1987

Stewart BW: Mechanisms of apoptosis: Integration of genetic, biochemical and cellular indicators. *J Natl Cancer Inst* 86:1286–1296, 1994

Ueda N, Shah SV: Apoptosis. *J Lab Clin Med* 124:169–177, 1994

Wahl SM: Transforming growth factor beta (TGF-β) in inflammation; a cause and a cure. *J Clin Immunol* 12:61–74, 1992

Wahl SM: Transforming growth factor β: the good, the bad, and the ugly. *J Exp Med* 180:1587–1590, 1994

Wahl SM, Hunt DA, Wakefield LM, McCartney-Francis N, Wahl LM, Roberts AB, Sporn MB: Transforming growth factor-β induces monocyte chemotaxis and growth factor production. *Proc Natl Acadsci USA* 84:5788–5792, 1987

Wang X, Smith P, Pu LL, Kirn YJ, Ko F, Robson MC: Exogenous transforming growth factor beta(2) modulates collagen I and collagen III synthesis in proliferative scar xenografts in nude rats. *J Surg Res* 87:194–200, 1999

Williams GT, Smith CA: Molecular regulation of apoptosis: Genetic controls on cell death. *Cell* 74:777–779, 1993

Yanagihara K, Tsumuraya M: Transforming growth factor β1 induces apoptotic cell death in cultured human gastric carcinoma cells. *Cancer Res* 52:4042–4045, 1992

Yang L, Qiu CX, Ludlow A, Ferguson MW, Brunner G: Active transforming growth factor-beta in wound repair: determination using a new assay. *Am J Pathol* 154:105–111, 1999

Yonish-Rouach E, Grunwald D, Wilder S, Kirnchi A, May E, Lawrence J-J, May P, Oren M: p53-Mediated cell death: relationship to cell cycle control. *Mol Cell Biol* 13:1415–1423, 1993